NACA

RESEARCH MEMORANDUM

INFLUENCE OF A CANARD-TYPE CONTROL SURFACE ON FLOW FIELD IN VICINITY OF SYMMETRICAL FUSELAGE AT MACH NUMBERS 1.8 AND 2.0

By George A. Wise and Murray Dryer

Lewis Flight Propulsion Laboratory
Cleveland, Ohio

NATIONAL ADVISORY COMMITTEE FOR AERONAUTICS

WASHINGTON
July 16, 1952

NATIONAL ADVISORY COMMITTEE FOR AERONAUTICS

RESEARCH MEMORANDUM

INFLUENCE OF A CANARD-TYPE CONTROL SURFACE ON FLOW FIELD IN VICINITY OF SYMMETRICAL FUSELAGE AT MACH NUMBERS 1.8 and 2.0

By George A. Wise and Murray Dryer

SUMMARY

An experimental investigation of the flow field downstream of a canard-type control surface and in the vicinity of a symmetrical body was conducted in the NACA Lewis 8- by 6-foot supersonic tunnel at Mach numbers of 1.8 and 2.0. Local stagnation pressures and flow deflection angles were measured 2.14 mean aerodynamic chord lengths downstream of the trailing edge of the control surface. A range of body angles of attack from 0° to 12° and control surface deflections of 0°, 5°, and 10° were investigated. Data were also obtained with the control surface removed.

The results indicated severe total pressure losses and large flow deflections in the control surface wake. A brief comparison of measured downwash with theory is made, and the effect of body sidewash on the location of the vortex cores is discussed.

INTRODUCTION

The behavior of the vortex system behind a lifting surface has been investigated both theoretically and experimentally by a number of investigators (references 1 to 6). It is pointed out in reference 4 that a knowledge of this flow field is essential for a rational approach to stability and control problems. Furthermore, if an air induction system is located in the disturbed flow region, the performance of the propulsion system may be penalized.

The investigation reported in reference 6 shows that the disturbances originating from a trapezoidal canard-type control surface still have considerable strength approximately 10 mean aerodynamic chord lengths downstream of the control surface. This investigation was extended to determine the characteristics of the flow field 2.14 mean aerodynamic chord lengths downstream of the trailing edge of a triangular cortrol surface and was performed in the NACA Lewis 8- by 6-foot supersonic tunnel at Mach numbers of 1.8 and 2.0

Total pressures and downwash angles were measured over a range of body angles of attack from 0° to 12° and at control surface deflection angles of 0°, 5°, and 10°. Data were also obtained with the control surface removed. The Reynolds number of the investigation was 3.8×10^6 based on the mean aerodynamic chord of the control surface.

SYMBOLS

The following symbols are used in this report:

A aspect ratio

b span of control surface

C_L coefficient of lift for control surface (linearized theory)

c chord

$\bar{c}$ mean aerodynamic chord $\dfrac{\int_0^{b/2} c^2\,dy}{\int_0^{b/2} c\,dy}$

H total pressure

M Mach number

s' distance between vortex cores

V_0 free-stream velocity

w downwash velocity (positive downward)

y distance measured horizontally from body axis

α angle of attack with respect to free-stream direction, deg

ε angle of downwash with respect to free-stream direction (positive downward), deg

δ canard deflection angle with respect to body axis

Subscripts:

0 free stream

1 local

B body

c control surface

2547

APPARATUS AND PROCEDURE

A sketch of the model is presented in figure 1(a), and details of the canard control surface are shown in figure 1(b). The fuselage was a body of revolution; and the control surface was a delta wing having raked tips, aspect ratio of 1.7, leading edge sweepback of 60°, and a dihedral of 15°.

The wake survey system, illustrated in figure 2, was located 22.27 inches or 2.14 mean aerodynamic chord lengths downstream of the trailing edge of the control surface. It was canted down at an angle of 5° to permit the wedges, which were limited in their useful angle of attack range, to operate from -5° to +7° instead of from 0° to 12°. Local Mach numbers and flow deflection angles were measured with the wedges, and the Mach numbers were used to correct the pitot pressures for normal shock losses. The total pressure ratios had an estimated accuracy of ±0.02 at points of measurement, and the maximum error in the downwash angles was estimated to be 0.5°. Duplicate runs were made with the survey system shifted laterally 1.25 inches in order to obtain Mach number data for each row of total tubes.

Boundary layer rakes were located circumferentially at $22\frac{1}{2}^{\circ}$ intervals around one-half of the fuselage with surface static orifices at each rake. A photograph showing the boundary layer rakes and the wake survey system mounted on the body is shown in figure 3.

RESULTS AND DISCUSSION

Experimental results. - The flow field around the body with the control surface removed is illustrated by means of total pressure ratio contours in figures 4 and 5 for Mach numbers of 1.8 and 2.0, respectively. A region of thickened boundary layer is indicated on the lee side of the body at angle of attack and becomes more pronounced with increasing angle of attack, finally resulting in separation. This is similar to the results of references 7 and 8. Measurements indicate negligible downwash outboard of a position 5.75 inches (or 1.54 body

radii) from the body axis in a horizontal direction; therefore, no downwash contours are included in figures 4 and 5.

The flow characteristics downstream of the control surface in the survey plane are presented in figures 6 to 10 for a Mach number of 1.8 and figures 11 to 15 for a Mach number of 2.0. It is indicated in figures 6 to 15 that, when the control surface was inclined to the free stream direction, a vortex was generated whose core was located in the vicinity of the streamwise projection of the tip of the control surface. Also, a region of lowered total pressure was propagated downstream, and the area of the region increased with increasing body and control surface angle of attack. It is also indicated that the formation of body cross-flow vortices (figs. 4 and 5) is inhibited by the presence of the control surface (figs. 10 and 15).

The downwash contours indicated a simple flow field consisting of essentially one main vortex at body angles of attack less than 9° (figs. 6 to 8 and 11 to 13) and indicated a more complex flow for body angles of attack of 9° and 12° (figs. 9, 10, 14, and 15), as noted from the more complex downwash contours. The origin of this more complex system possibly lies in the interaction of the body cross flow with the vortex sheet generated by the control surface.

A comparison of figures 6 to 10 with figures 11 to 15 indicates that the same type flow occurred at both Mach numbers.

Comparison with theory. - The spanwise locations of the vortex cores, as measured by assuming that the core lies on the imaginary zero line of the downwash contours, are shown in figure 16 for the range of control surface angles of attack at $M_0 = 1.8$ and 2.0. Included for comparison with available theory (reference 2) are the theoretical asymptotic spacings of the vortex cores which trail behind (a) an elliptical wing having elliptical loading and (b) a triangular wing as calculated from experimental span loadings. Thus it must be remembered that the experimental model differs from the theoretical model in the following respects: (a) The experimental span loading is neither elliptical nor can it be assumed to be that of the triangular wing of reference 2, as a consequence of the control surface dihedral, raked tips, aspect ratio of 1.7, gap effects, and the presence of the symmetrical fuselage; and (b) the experimental data are significantly affected by the presence of the body, while the theory is for a wing alone. Although the asymptotic spacings for the control surface vortex cores are not known, it is believed that, for $M_0 = 2.0$ and $\delta = 0^\circ$, the core locations at $\alpha_c > 10^\circ$ are close to those which would be determined by several downstream survey stations. Thus, agreement of the experimental vortex core locations with those for the triangular wing occurs within 5 to 10 percent of the spanwise distance for the range

$8^\circ < \alpha_c < 12^\circ$. The core locations for $\delta = 5^\circ$ also agree within 5 to 10 percent for the range of α_c between 12° and 16°. For $\delta = 10^\circ$, however, there is no agreement probably as a result of (a) body cross flow effects, (b) secondary effects due to vortices forming behind the projecting root chord leading edge, or (c) flow separation on the control surface.

The effect of the body cross flow on the core locations is particularly noted at $\delta = 0^\circ$ and 5° at $M_0 = 2.0$. For example, the spanwise core location at $\delta = 0^\circ$ and $\alpha_B = 10^\circ$ (that is, $\alpha_c = 10^\circ$) is at $s'/b = 0.85$; whereas, at $\delta = 5^\circ$ and $\alpha_B = 5^\circ$, $s'/b = 0.95$. In the latter case, the cores are prevented from moving inboard by the body sidewash; in the former case, the vortex cores are above most body flow disturbances. The schlieren photographs (fig. 17) at $M_0 = 2.0$ and $\delta = 0^\circ$ illustrate this movement of the vortex cores above the body with increasing α_B.

The effect of the sidewash was further investigated in the following manner: from water tank measurements of a triangular wing alone (reference 2) the vortex core location was approximated (at a station corresponding to that investigated herein) to be $s'/b = 0.90$ at $\alpha_c = 3^\circ$. The 10 percent movement to $s'/b = 0.99$ for the core behind the control surface at $M_0 = 2.0$ and $\alpha_c = 3^\circ$ (fig. 16) was compared with the deviation of a streamline which passes through a point corresponding to the tip of the control surface as calculated by linearized theory for the body alone at $\alpha_B = 0^\circ$. The two deviations are of equal magnitude, indicating that vortex core spanwise locations might be predicted at low angles of attack by using body potential sidewash to correct the locations indicated in reference 2.

In order to obtain some insight as to the trends and magnitudes of the downwash angles and how they compare with theory, downwash measurements at $M_0 = 2.0$ and $\delta = 0^\circ$ were taken from the contours for $\alpha_B = 3^\circ$, 6°, 9°, and 12° (figs. 12(a), 13(a), 14(a), and 15(a), respectively). With the use of theoretical linearized lift coefficients, the downwash angles are presented in figure 18 in the form $\frac{w}{V_0}\frac{\pi A}{C_L}$ against $\frac{2y}{b}$, where $\frac{w}{V_0} = \tan \varepsilon$. For comparison, theoretical downwash values (reference 2) are shown for a simple triangular wing (having the same values of C_L and A) whose cores are assumed to be located in the same spanwise location given by the triangular wing in figure 16 at $\alpha_c \leq 12^\circ$, that is, $s'/b = 0.79$. Since the experimental vortex cores are in different spanwise locations (fig. 16), no direct quantitative comparison can be made. A qualitative comparison of theoretical and experimental downwash angles, however, is satisfactory if the experimental vortex cores are assumed to be translated to the

theoretical core location, $s'/b \approx 0.79$. For instance, if the curve for $\alpha_B = 3^\circ$ (fig. 18) were translated to the left, good agreement with theory would result. This agreement, useful for preliminary engineering studies, becomes less satisfactory inboard of the vortex core as the body angle of attack is increased because of (a) interference effects between the body cross flow and the vortex sheet, and (b) the difference between experimental and theoretical vortex strengths as measured by the maximum ordinates of the downwash curves. The good agreement that otherwise occurs (assuming translation of the core as already suggested) is interesting in view of the fact that experimental results were obtained using a body-wing combination with a wing (or control surface) having dihedral and raked tips, whereas theoretical results considered the completely rolled-up vortex sheet far behind a simple triangular wing.

CONCLUDING REMARKS

An investigation at Mach numbers of 1.8 and 2.0 of the flow field located 2.14 mean aerodynamic chord lengths behind a canard-type control surface and in the vicinity of a symmetrical fuselage indicated the following:

1. A disturbed region of severe total pressure losses and large flow angularities was propagated downstream in a streamwise direction of the trailing edge of the control surface. This region increased in area with increased inclination of the control surface to the free stream flow. Starting at about a 9° body angle of attack, a more complex flow was noted, possibly as a result of interaction of the body cross flow with the vortex sheet generated by the control surface. Location of an engine inlet, lifting surface, or stabilizing surface would therefore necessitate consideration of these adverse flow conditions.

2. A brief qualitative comparison of theoretical and experimental downwash angles showed good agreement at the low body angles of attack with zero control surface deflection, assuming identical theoretical and experimental vortex core locations.

Lewis Flight Propulsion Laboratory
National Advisory Committee for Aeronautics
Cleveland, Ohio

REFERENCES

1. Westwater, F. L.: Rolling Up of the Surface of Discontinuity Behind an Aerofoil of Finite Span. R. & M. No. 1692, British A.R.C., 1936.

2. Spreiter, John R., and Sacks, Alvin H.: The Rolling Up of the Trailing Vortex Sheet and Its Effect on the Downwash Behind Wings. Jour. Aero. Sci., vol. 18, no. 1, Jan. 1951, pp. 21-32, 72.

3. Wetzel, Benton E., and Pfyl, Frank A.: Measurements of Downwash and Sidewash Behind Cruciform Triangular Wings at Mach Number 1.4. NACA RM A51B20, 1951.

4. Spreiter, John R.: Downwash and Sidewash Fields Behind Cruciform Wings. NACA RM A51L17, 1952.

5. Sacks, Alvin H.: Behavior of Vortex System Behind Cruciform Wings - Motions of Fully Rolled-up Vortices. NACA TN 2605, 1952.

6. Fradenburgh, Evan A., Obery, Leonard J., and Mello, John F.: Influence of Fuselage and Canard-Type Control Surface on the Flow Field Adjacent to a Rearward Fuselage Station at a Mach Number of 2.0 - Data Presentation. NACA RM E51K05, 1952.

7. Luidens, Roger W., and Simon, Paul C.: Aerodynamic Characteristics of NACA RM-10 Missile in 8- by 6-Foot Supersonic Wind Tunnel at Mach Numbers from 1.49 to 1.98. I - Presentation and Analysis of Pressure Measurements (Stabilizing Fins Removed). NACA RM E50D10, 1950.

8. Allen, H. Julian, and Perkins, Edward W.: Characteristics of Flow Over Inclined Bodies of Revolution. NACA RM A50L07, 1951.

2547

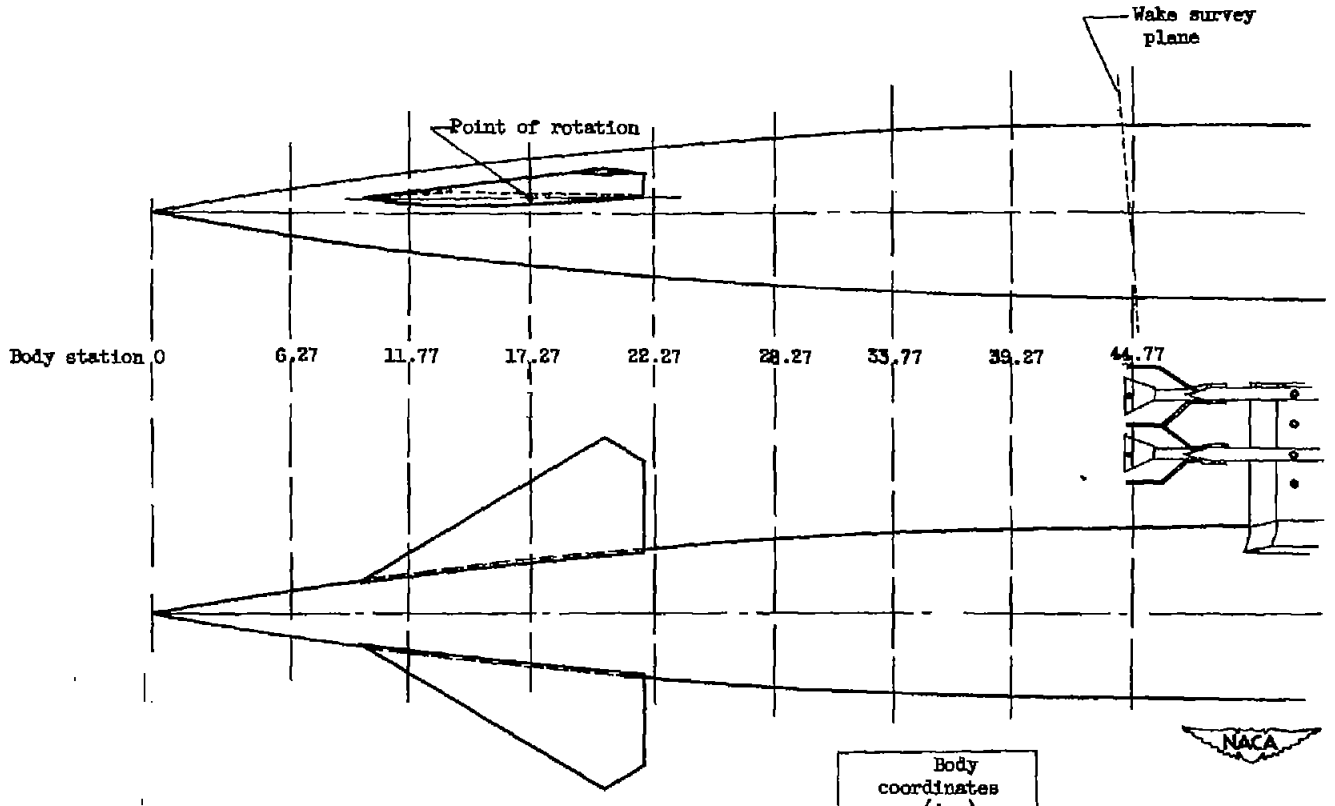

Body coordinates (in.)	
Station	Diameter
0	0
6.27	1.94
11.77	3.42
17.27	4.64
22.77	5.67
28.27	6.46
33.77	7.02
39.27	7.36
44.77	7.48

(a) Forward body assembly.

Figure 1. - Test model.

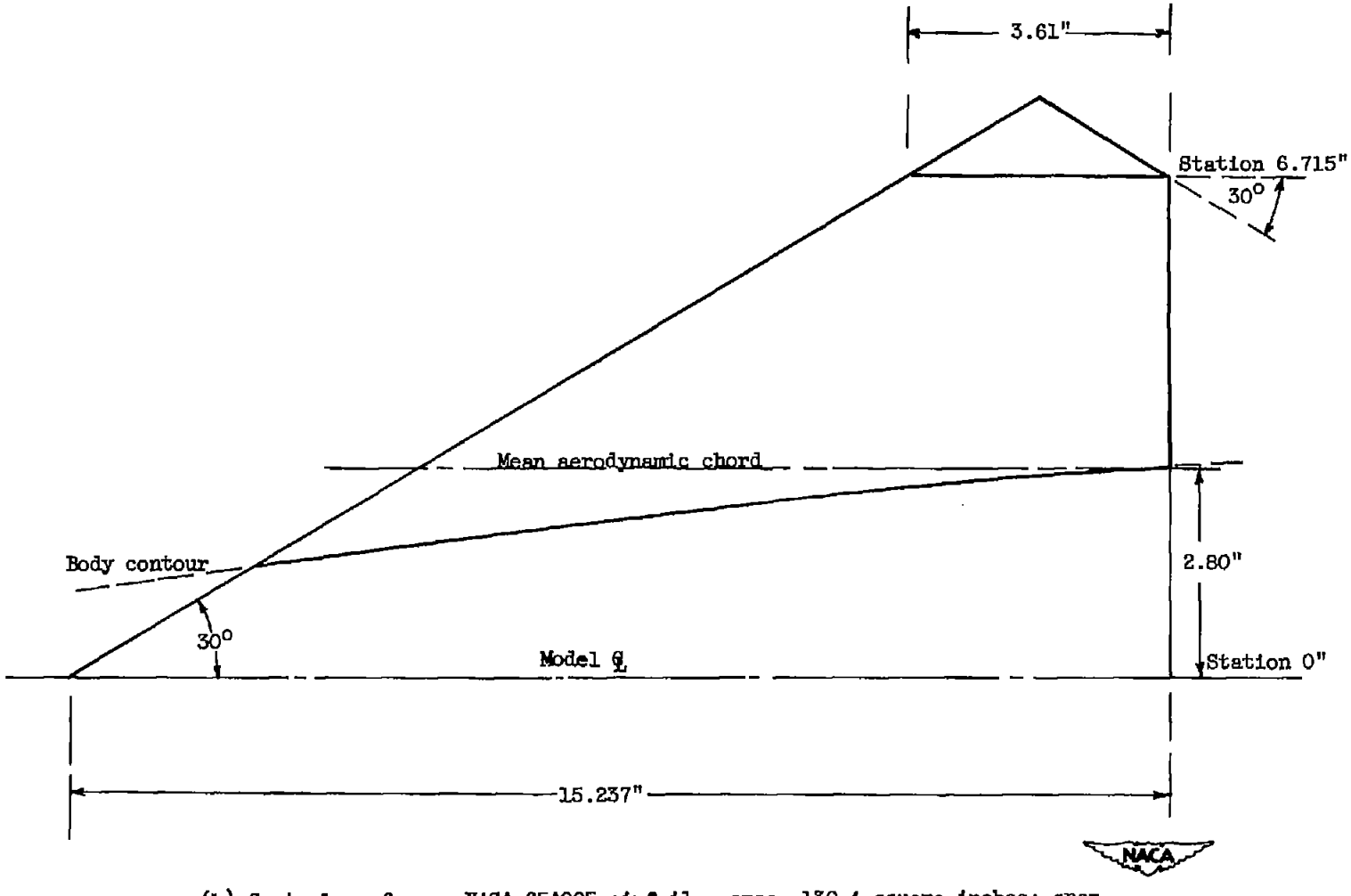

(b) Control surface. NACA 65A005 airfoil: area, 130.4 square inches; span, 14.99 inches; mean aerodynamic chord, 10.4 inches; aspect ratio, 1.7; dihedral, 15°.

Figure 1. - Concluded. Test model.

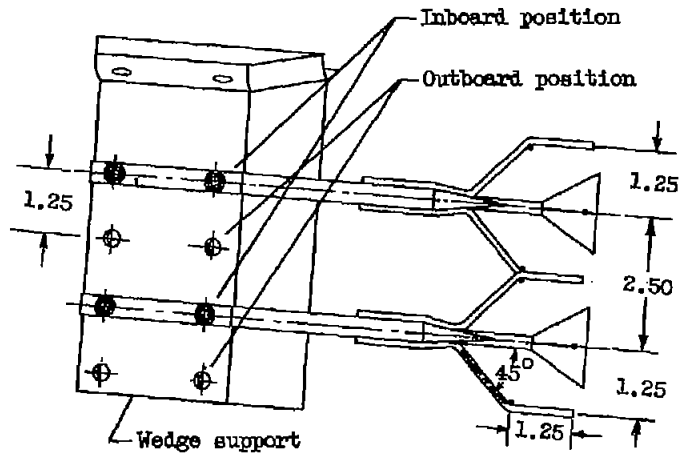

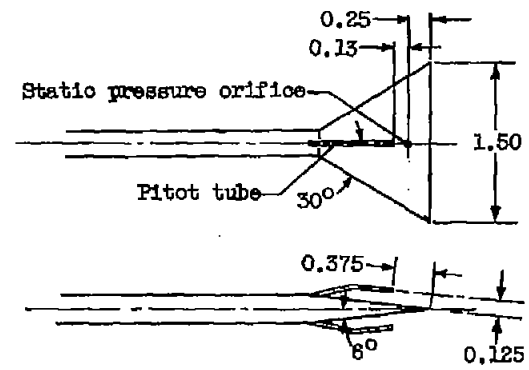

Details of wedge

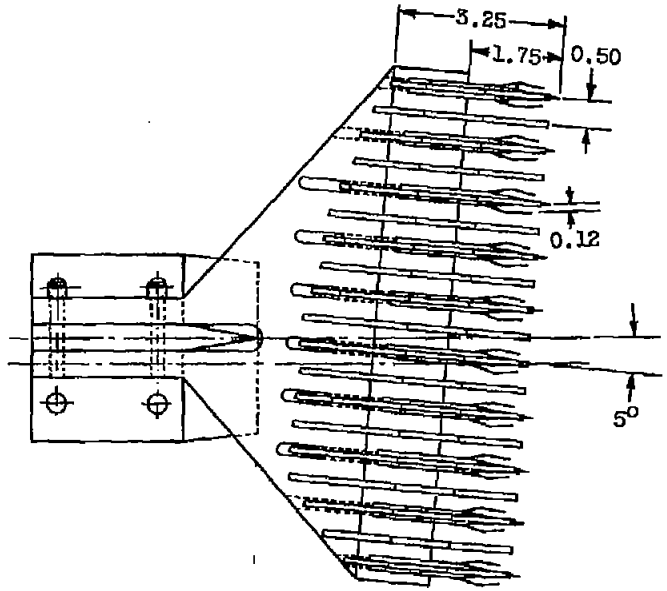

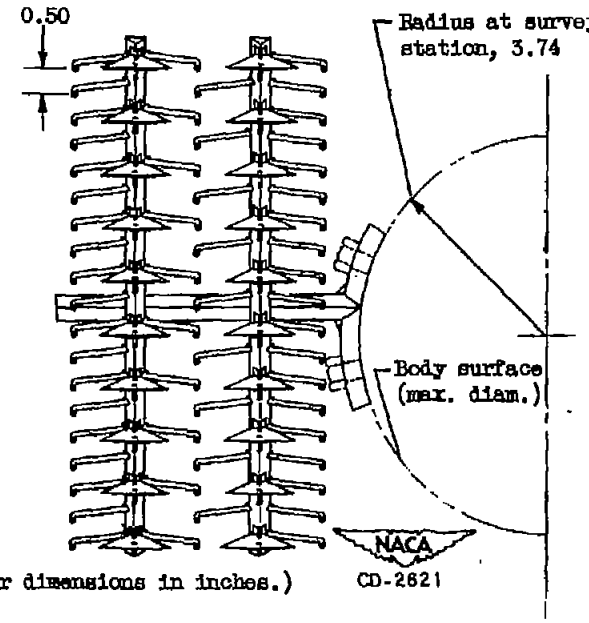

Figure 2. - Survey rake. (All linear dimensions in inches.)

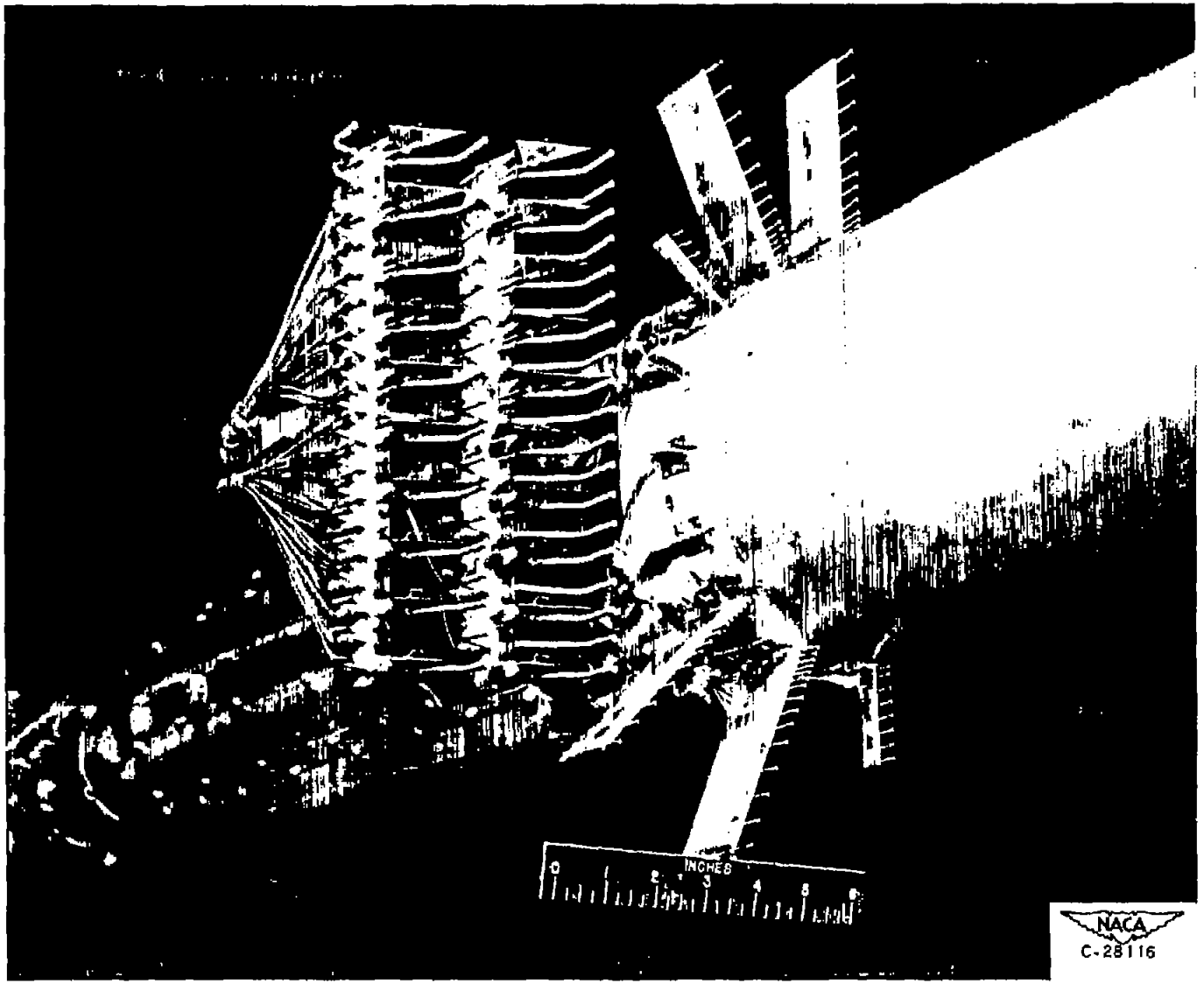

Figure 3. - Wake survey instrumentation.

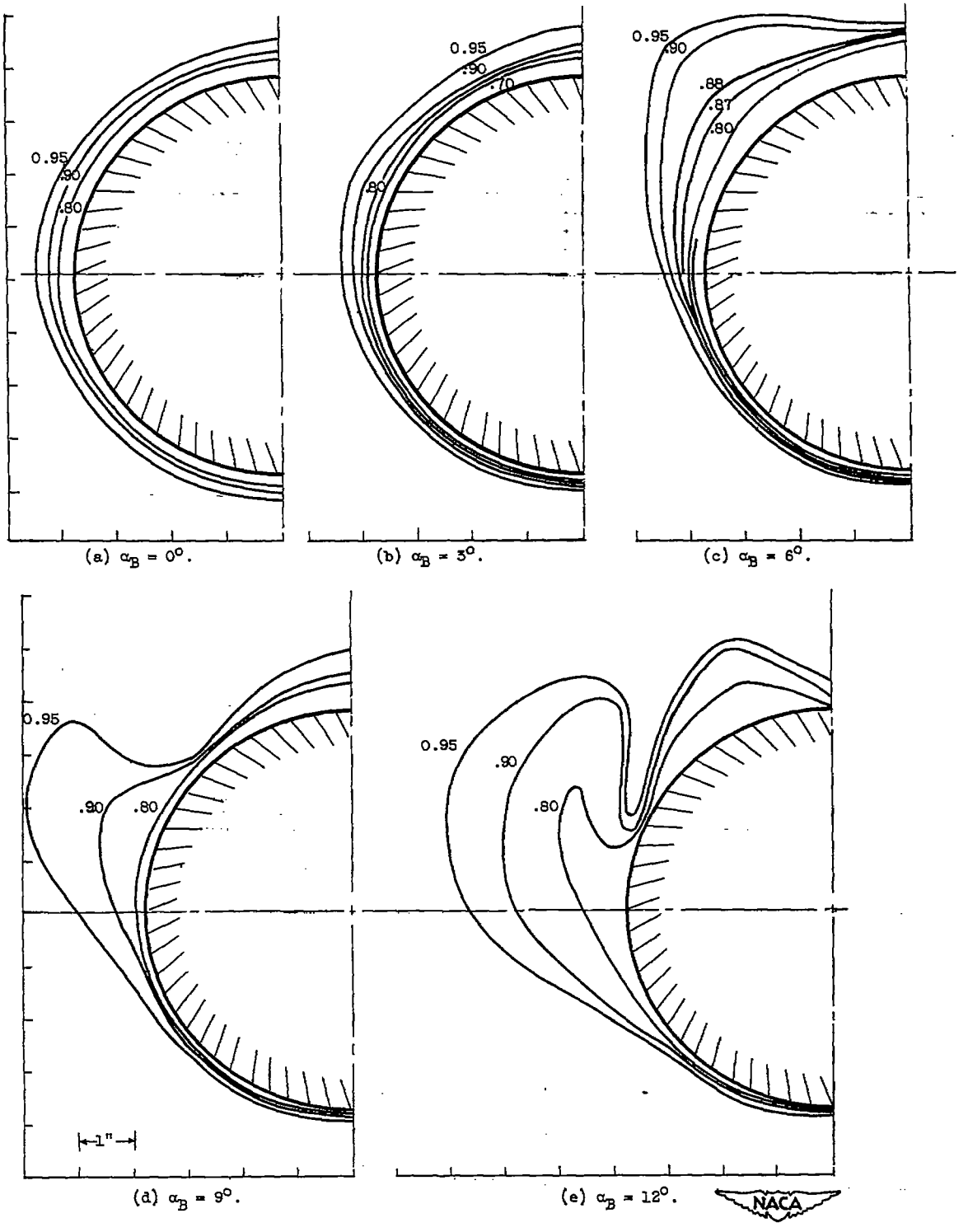

Figure 4. - Contours of total pressure ratio H_1/H_0 at station 44.66 and Mach number M_0 of 1.8. Canard control surface removed.

[redacted]

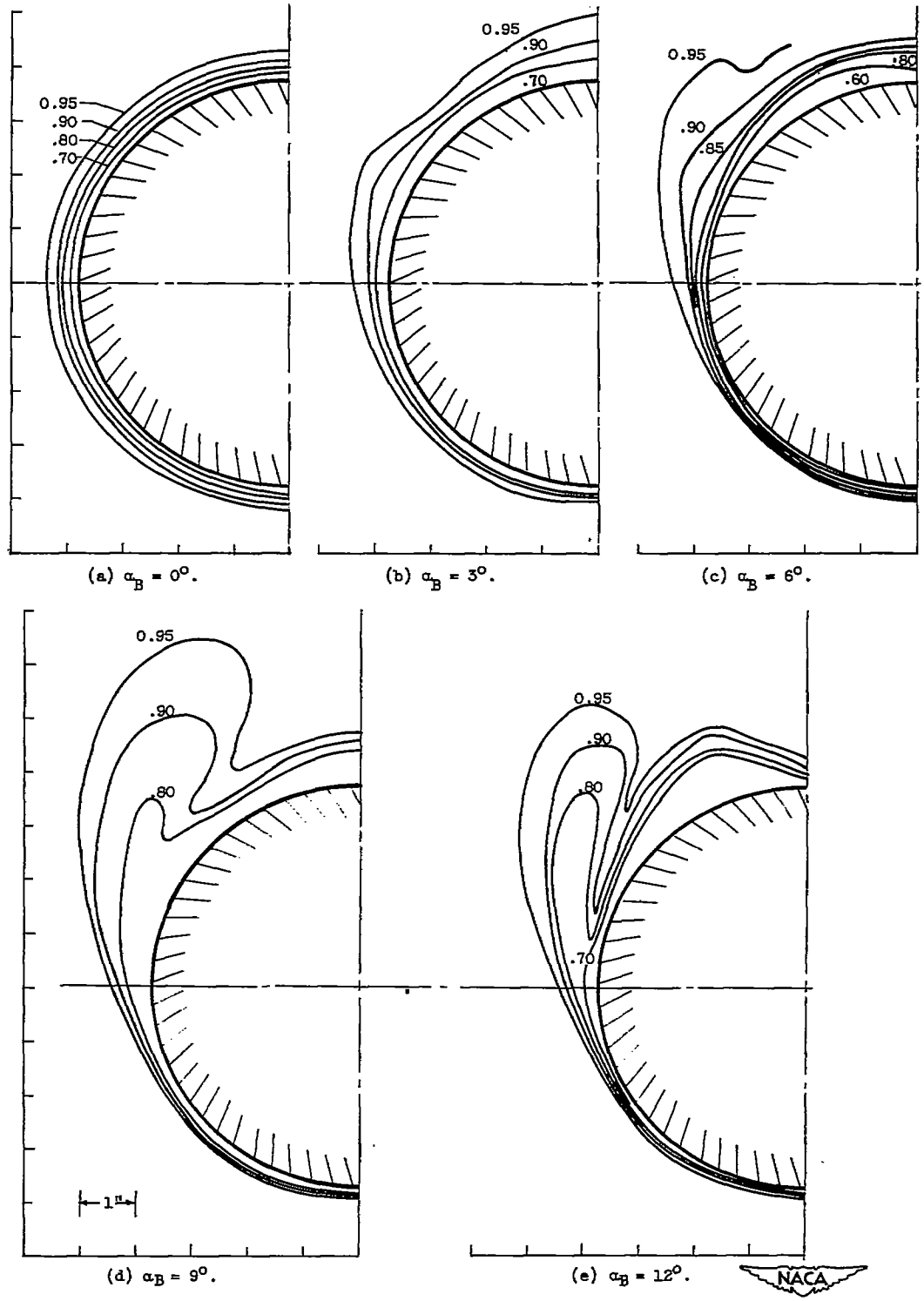

Figure 5. - Contours of total pressure ratio H_1/H_0 at station 44.66 and Mach number M_0 of 2.0. Canard control surface removed.

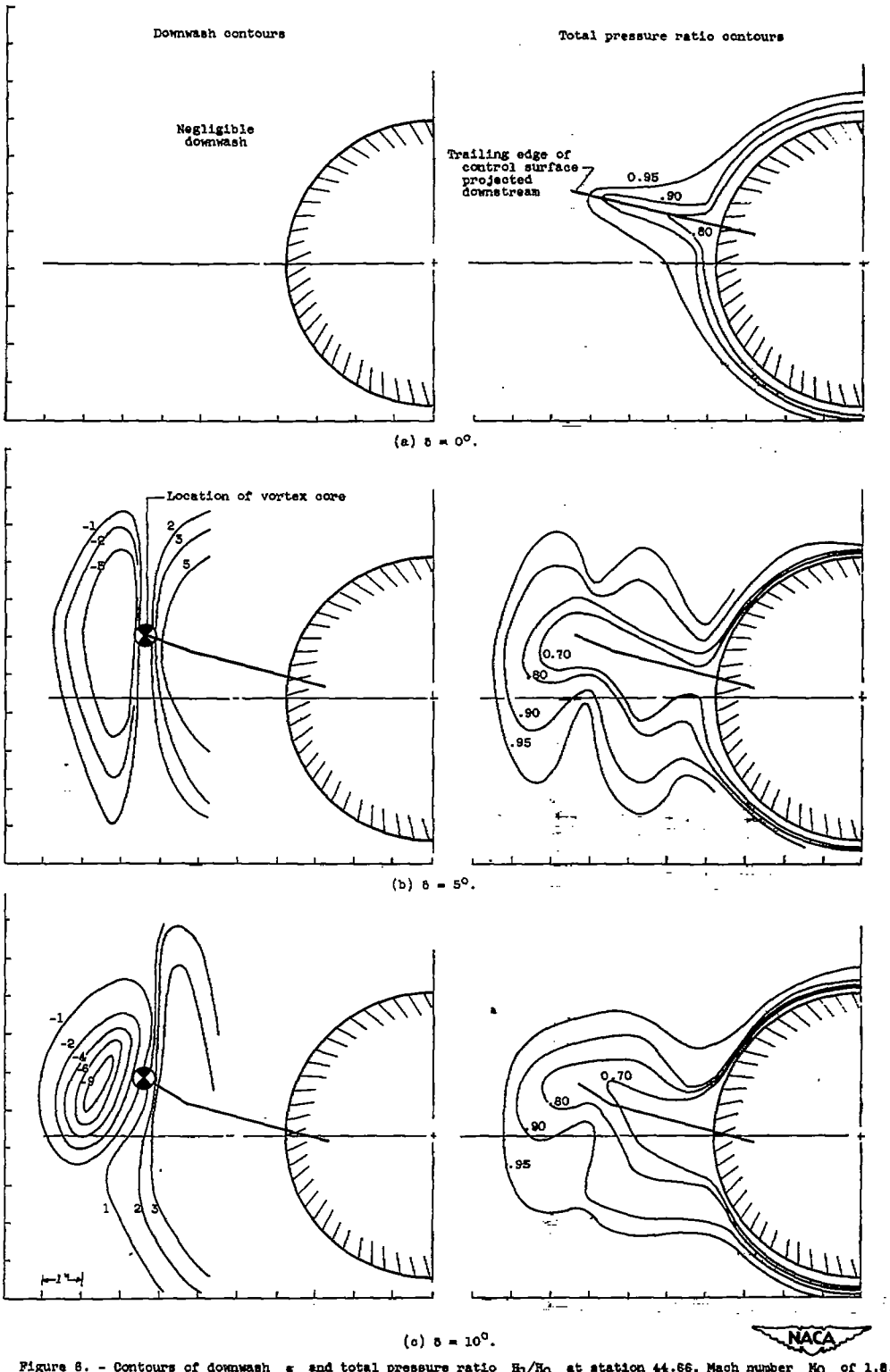

Figure 8. - Contours of downwash ϵ and total pressure ratio H_1/H_0 at station 44.66, Mach number M_0 of 1.8, and body angle of attack α_B of 0°.

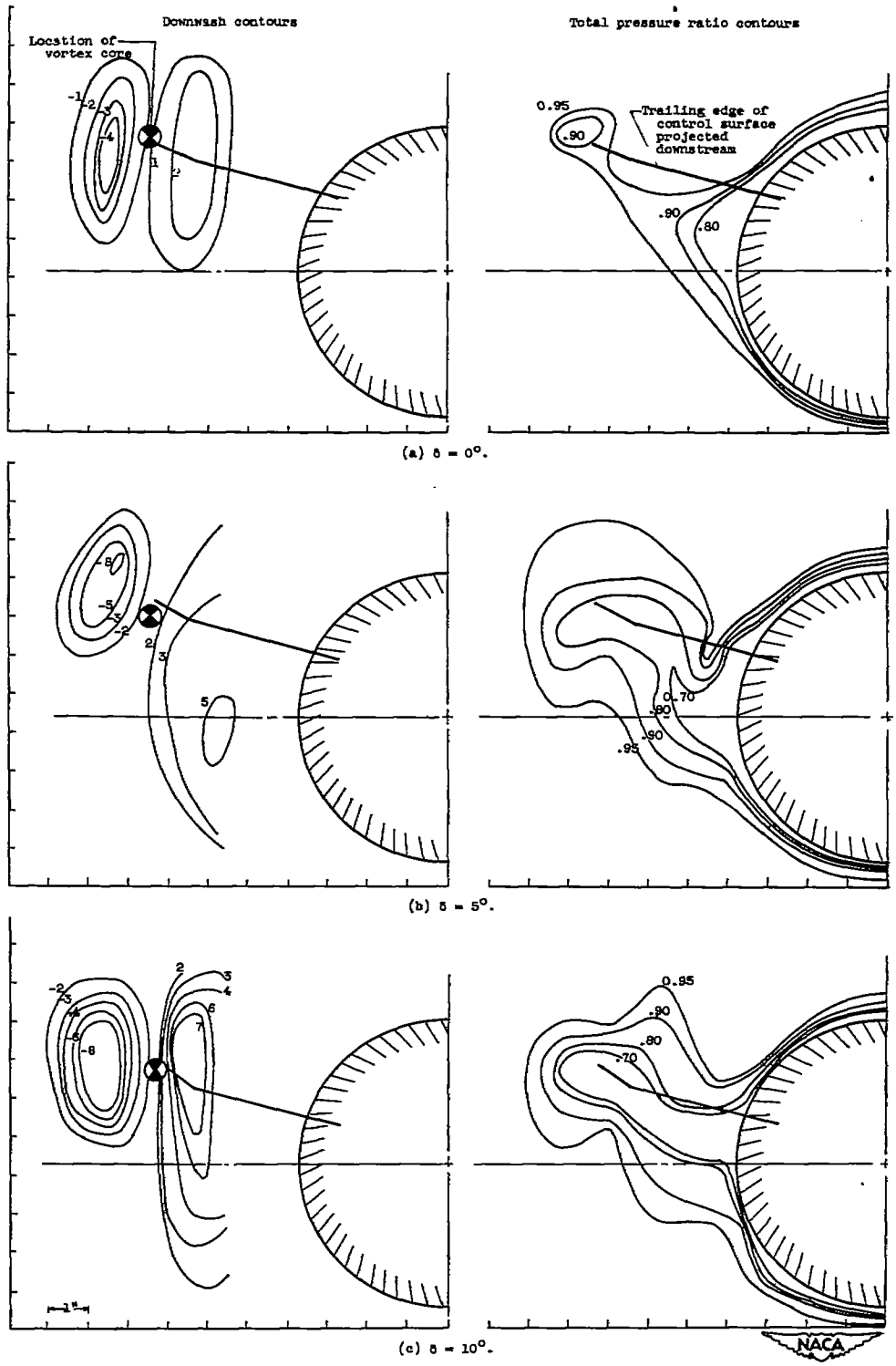

(a) $\delta = 0°$.

(b) $\delta = 5°$.

(c) $\delta = 10°$.

Figure 7. - Contours of downwash ε and total pressure ratio H_1/H_0 at station 44.66, Mach number M_0 of 1.8, and body angle of attack α_B of 3°.

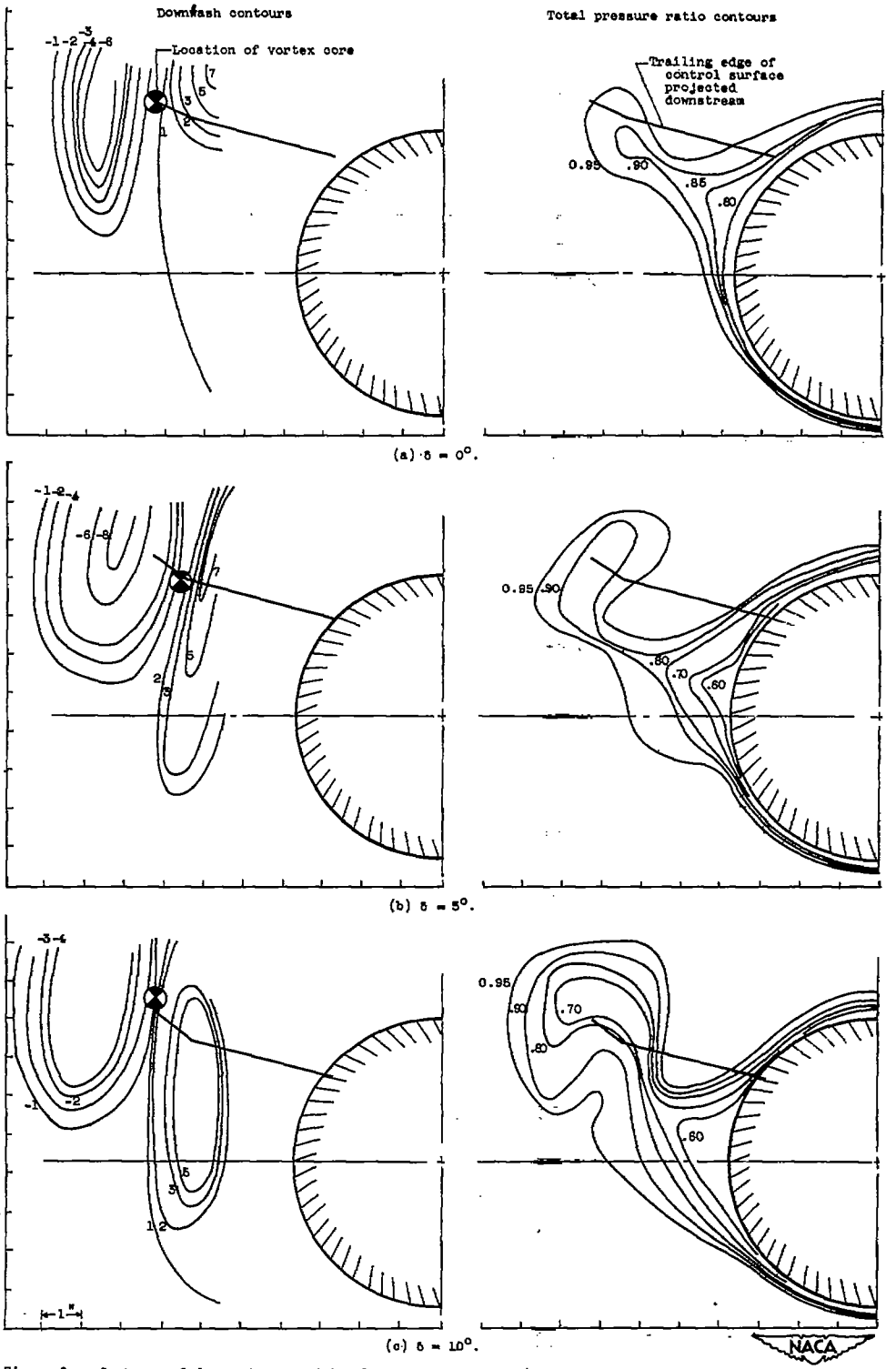

Figure 8. - Contours of downwash ε and total pressure ratio H_1/H_0 at station 44.88, Mach number M_0 of 1.8, and body angle of attack α_B of 6°.

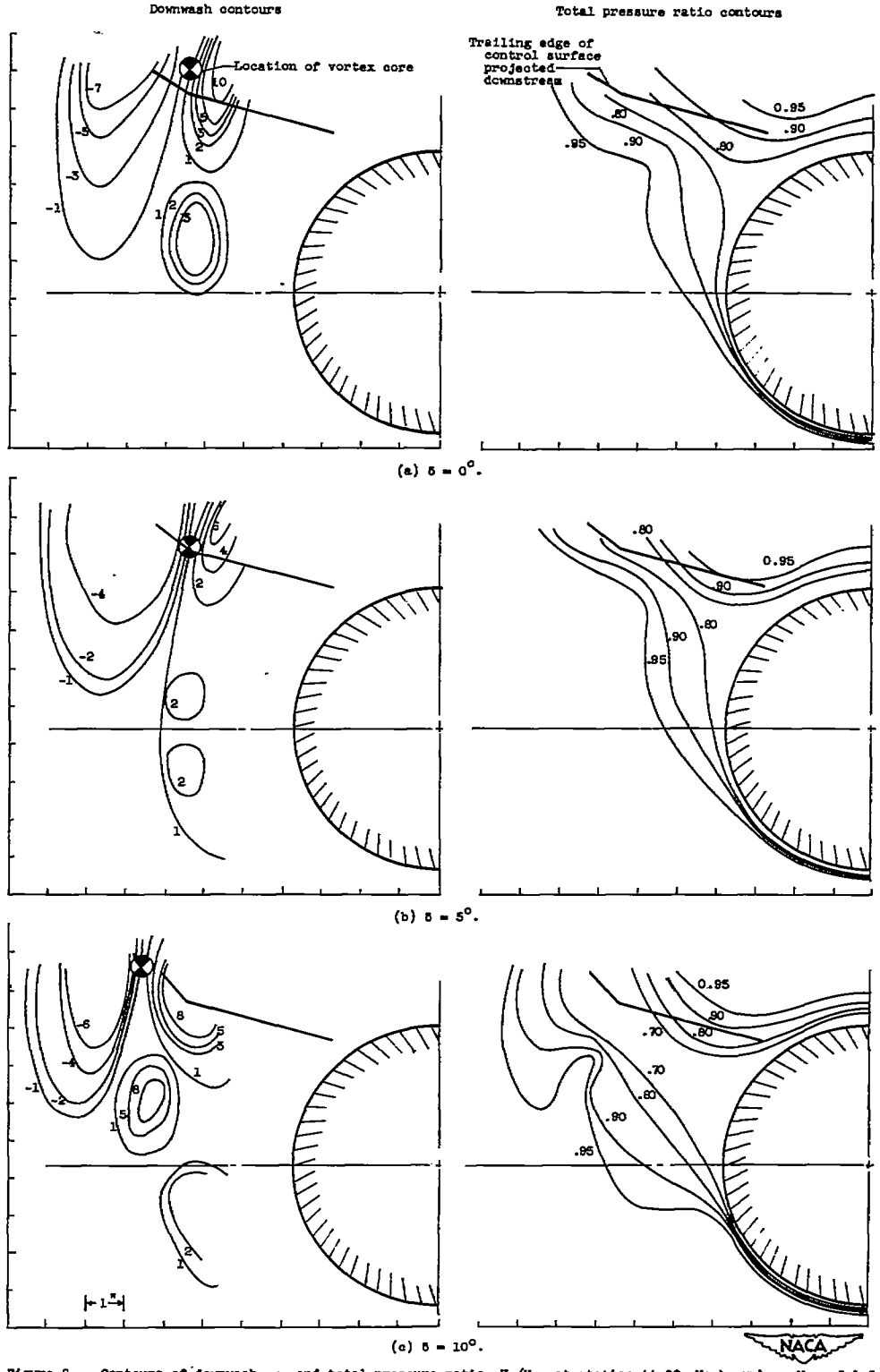

Figure 9. - Contours of downwash ε and total pressure ratio H_1/H_0 at station 44.66, Mach number M_0 of 1.8, and body angle of attack α_B of 9°.

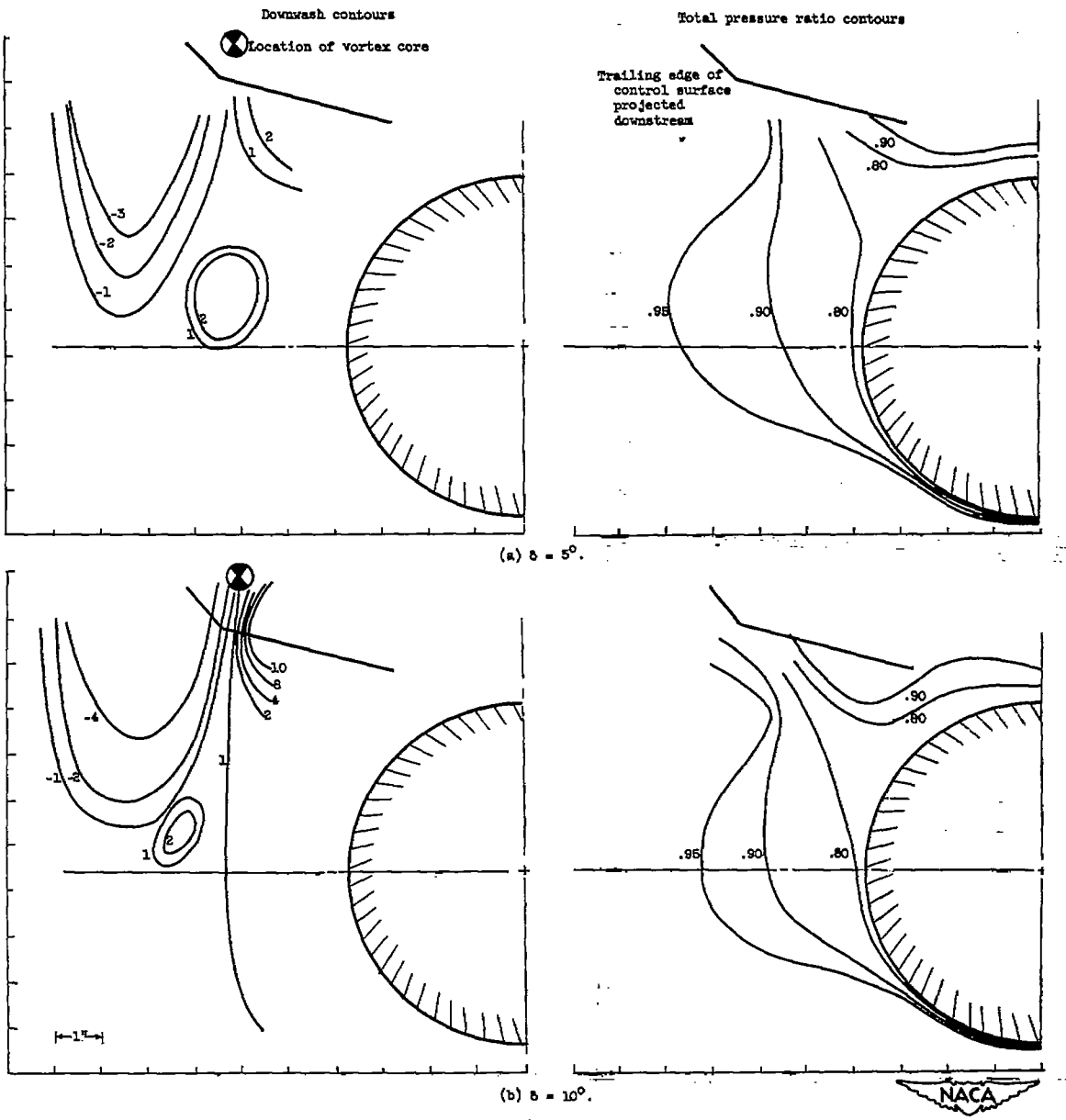

Figure 10. - Contours of downwash ε and total pressure ratio H_1/H_0 at station 44.66, Mach number M_0 of 1.8, and body angle of attack α_B of 12°. (Data not obtained for $\delta = 0$.)

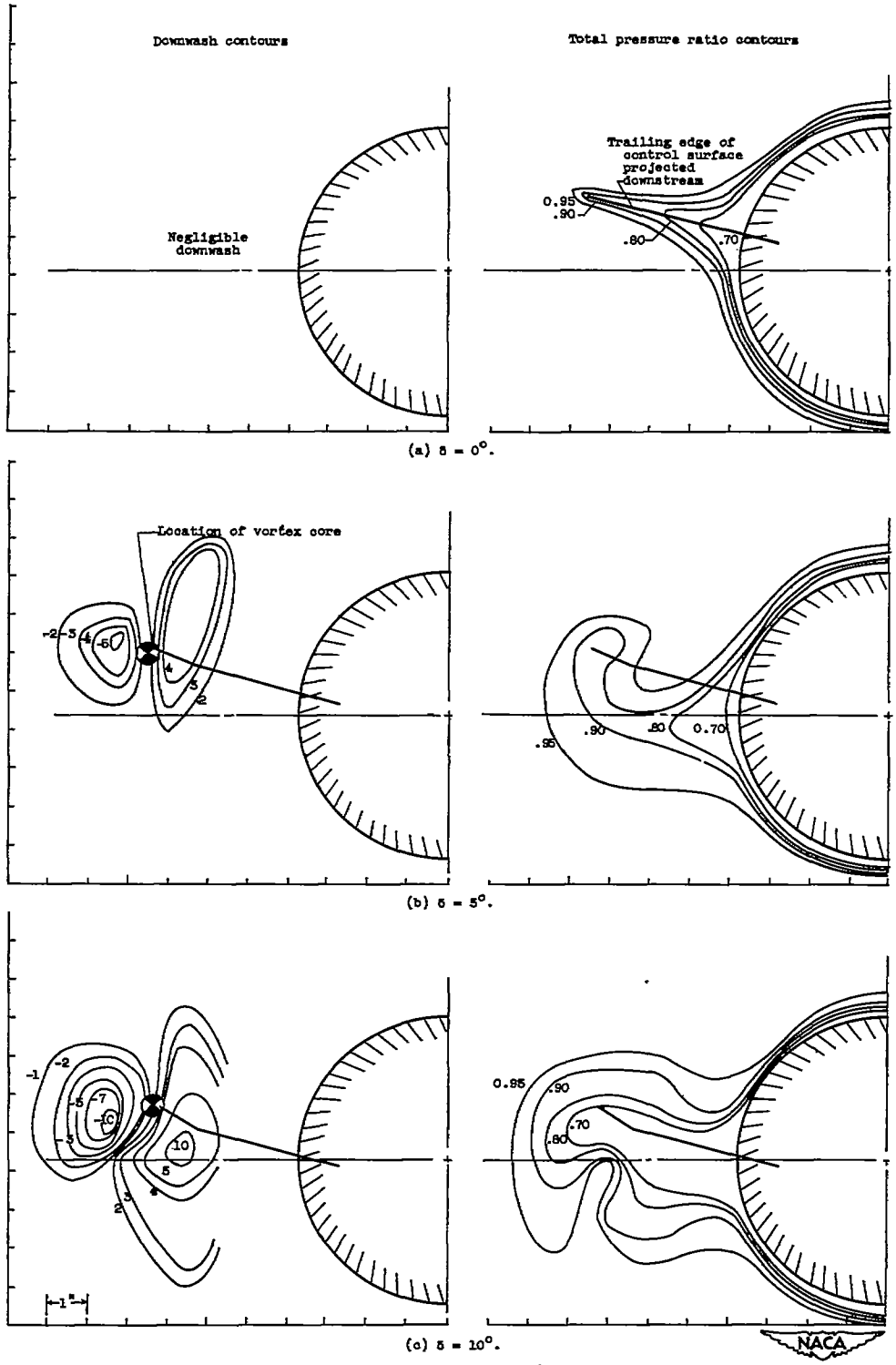

Figure 11. - Contours of downwash ϵ and total pressure ratio H_1/H_0 at station 44.66, Mach number M_0 of 2.0, and body angle of attack α_B of 0°.

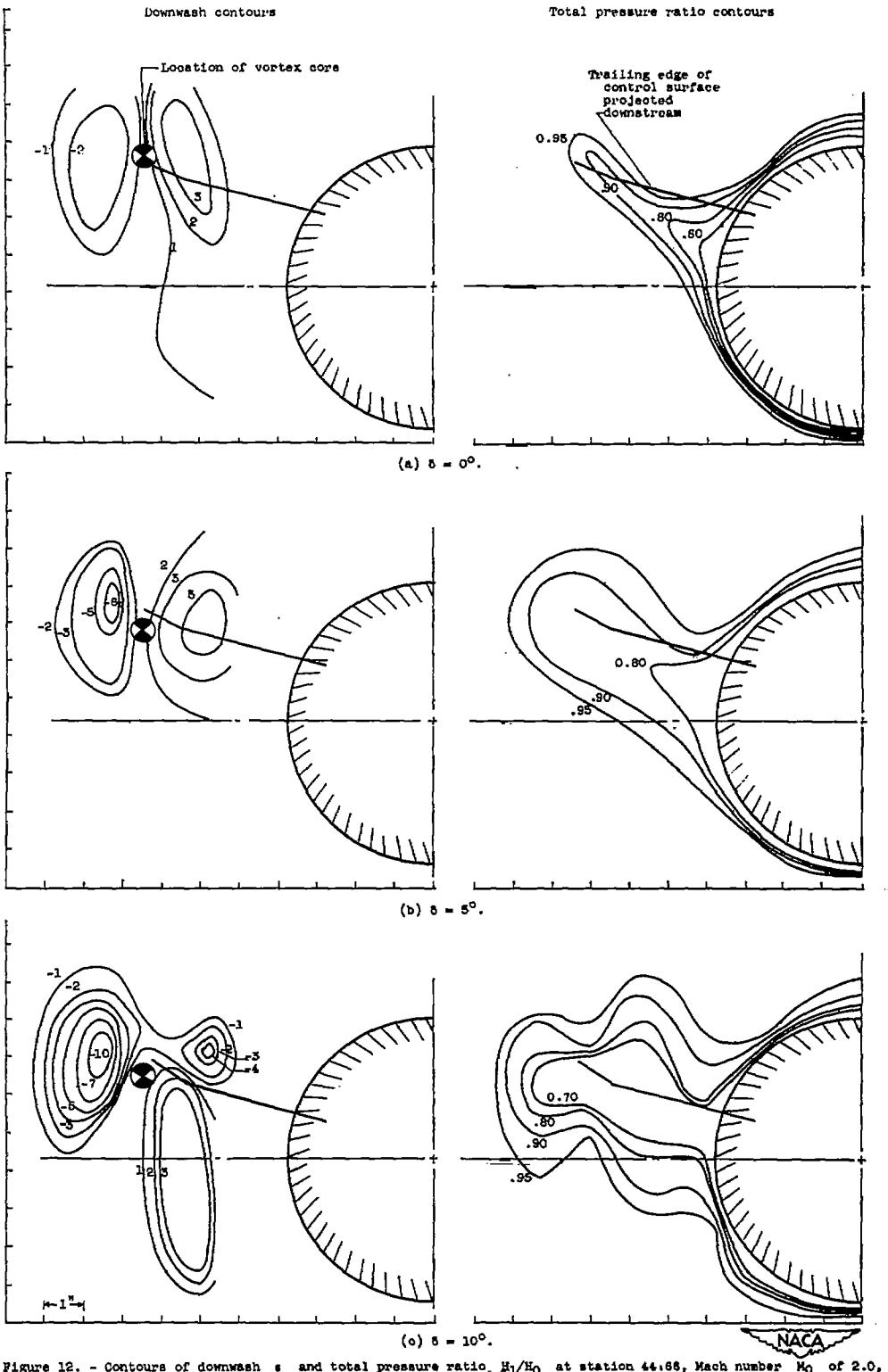

Figure 12. - Contours of downwash ϵ and total pressure ratio H_1/H_0 at station 44.66, Mach number M_0 of 2.0, and body angle of attack α_B of 5°.

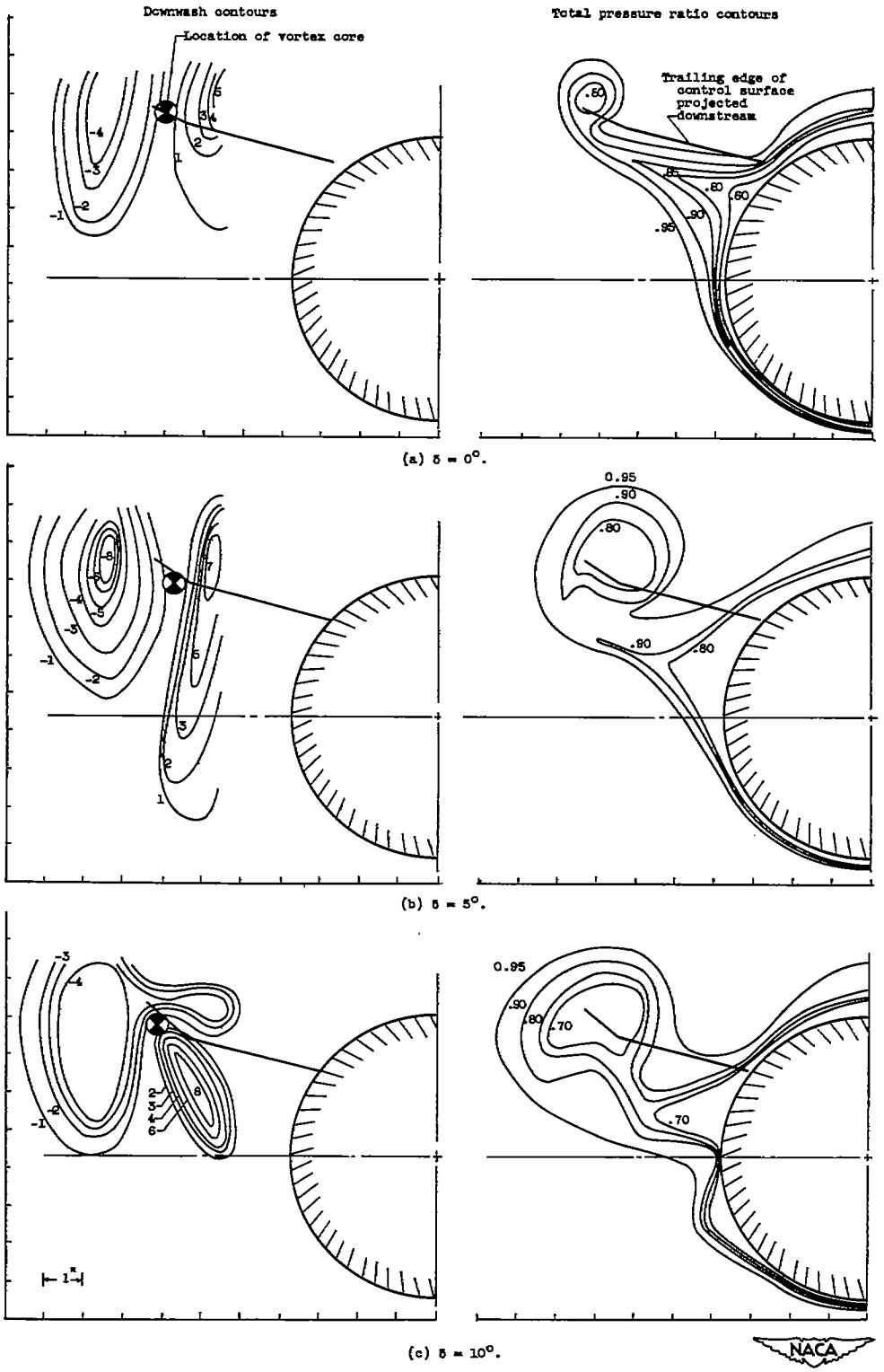

Figure 13. - Contours of downwash ε and total pressure ratio H_1/H_0 at station 44.66, Mach number M_0 of 2.0, and body angle of attack α_B of 8°.

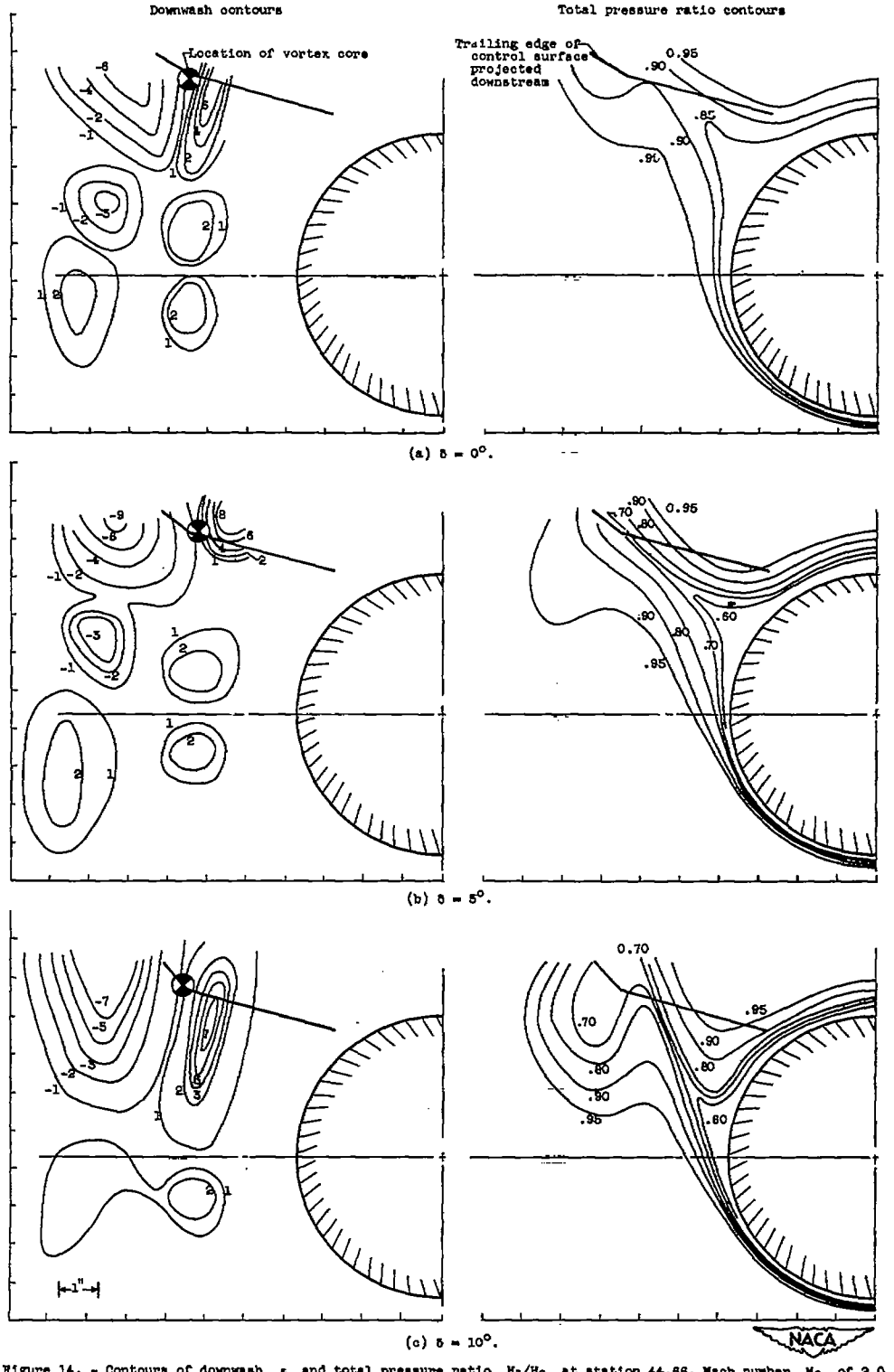

Figure 14. - Contours of downwash ϵ and total pressure ratio H_1/H_0 at station 44.66, Mach number M_0 of 2.0, and body angle of attack α_B of 9°.

[redacted]

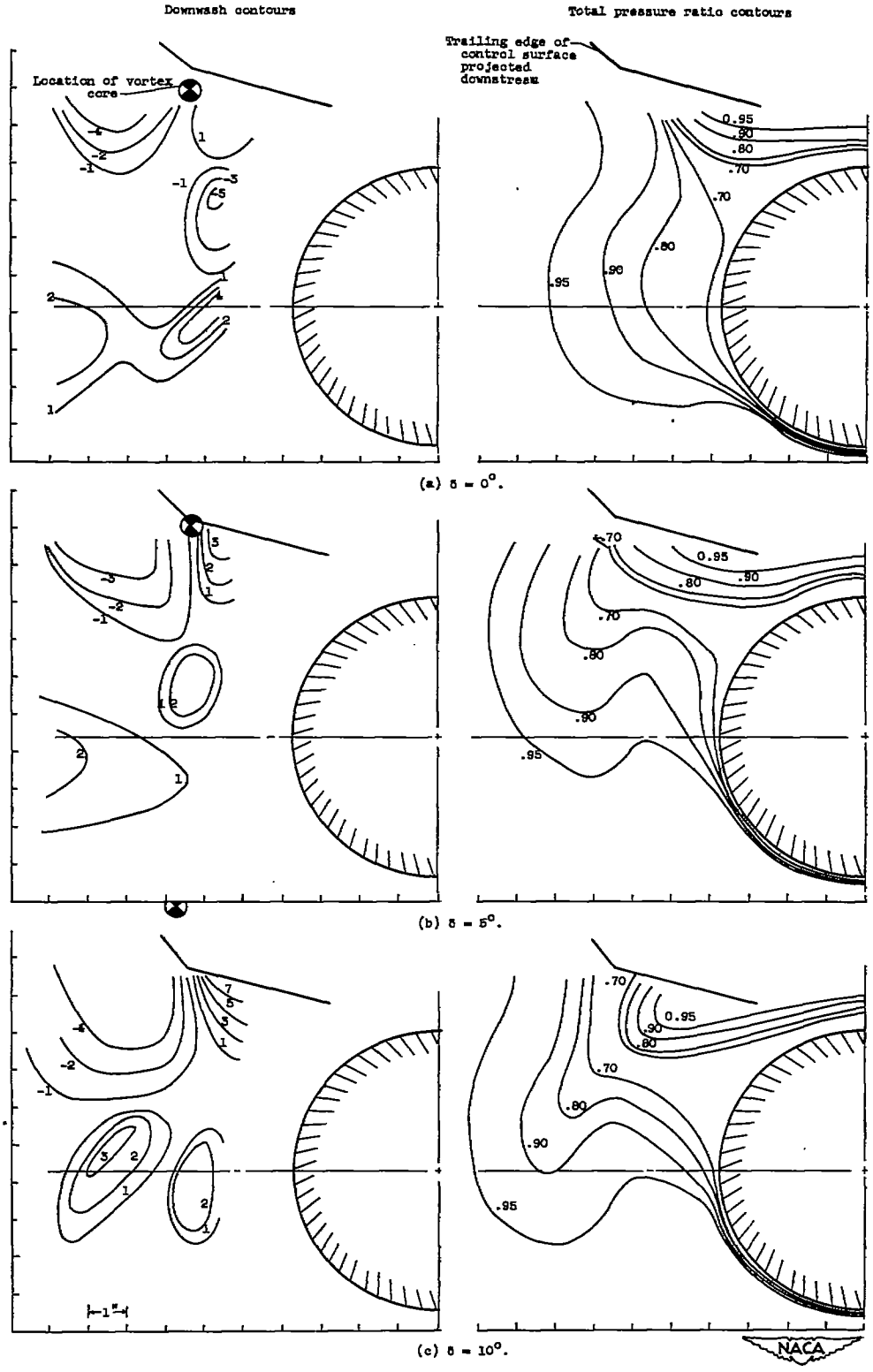

Figure 15. - Contours of downwash ε and total pressure ratio H_1/H_0 at station 44.66, Mach number M_0 of 2.0, and body angle of attack α_B of 12°.

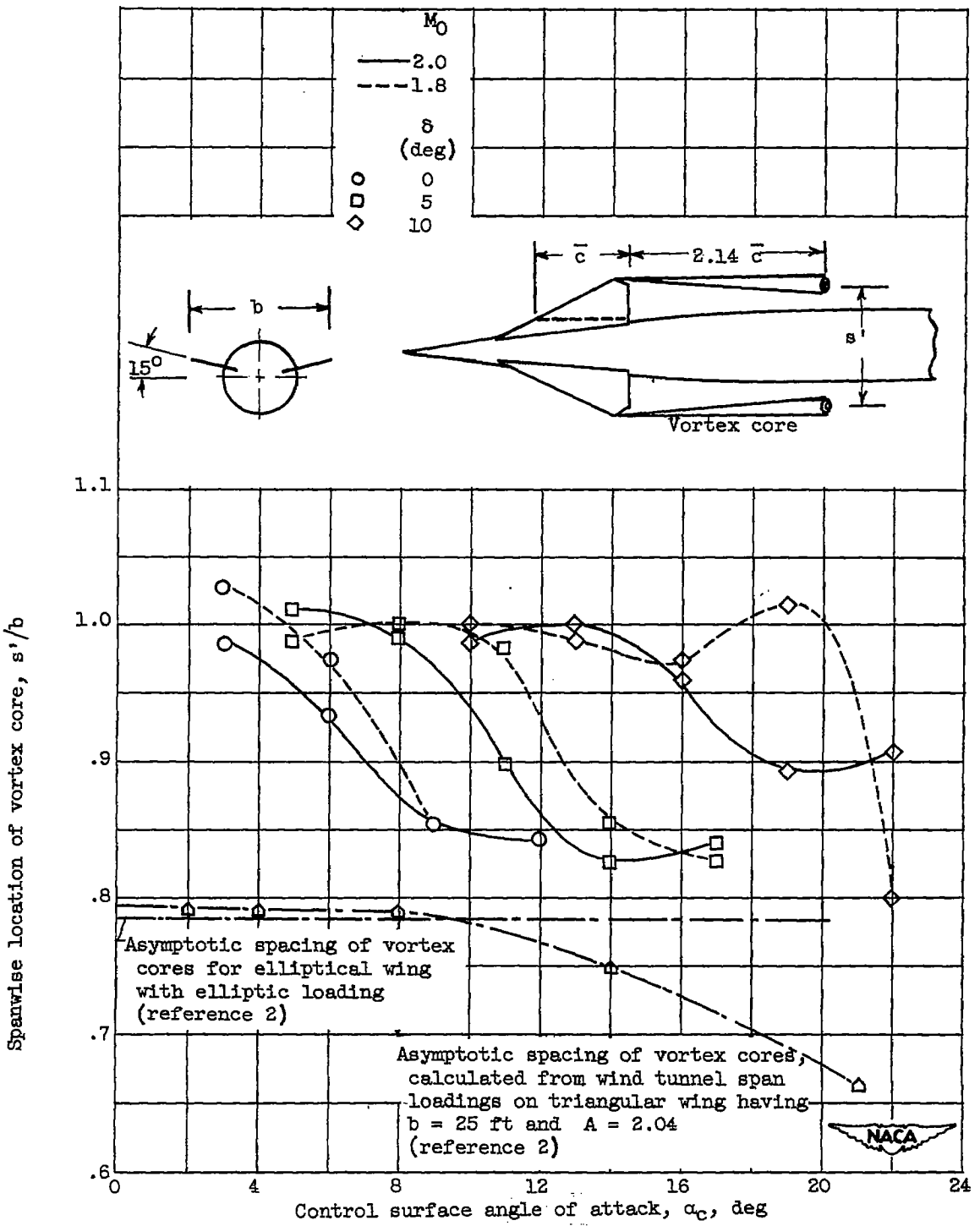

Figure 16. - Spanwise location of vortex cores downstream of a triangular control surface of aspect ratio 1.7 at distance of 2.14 mean aerodynamic chord lengths downstream of trailing edge.

[redacted]

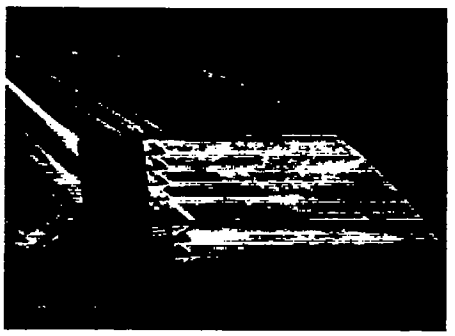

(a) $\alpha_B = 6^\circ$.

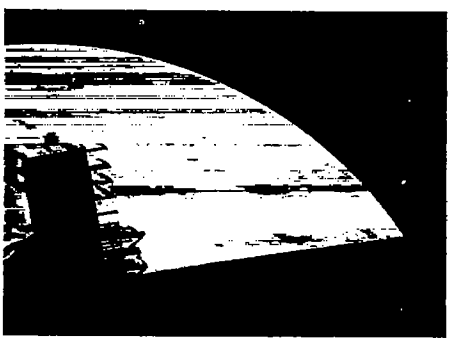

(b) $\alpha_B = 9^\circ$.

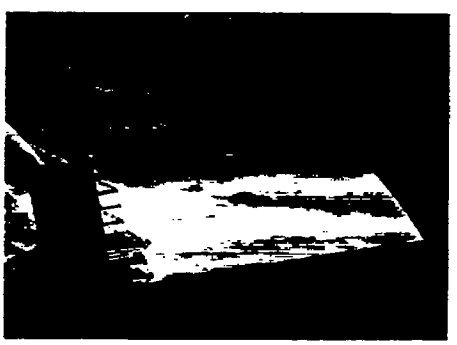

NACA
C-29682

(c) $\alpha_B = 12^\circ$.

Figure 17. - Schlieren photographs of vortex wake downstream of canard control surface. M_0, 2.0; δ, 0°.

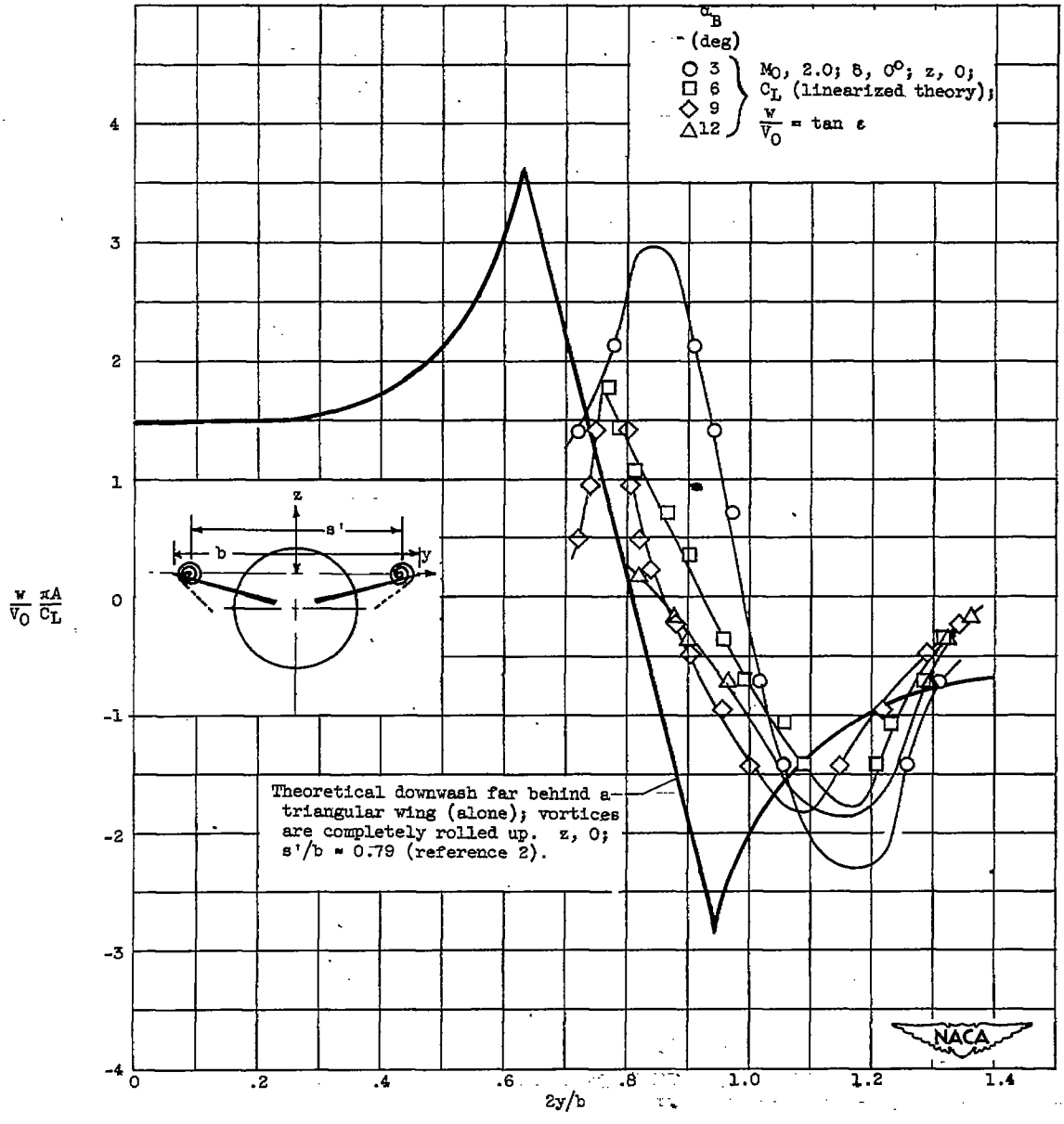

Figure 18. - Comparison between experimental and theoretical downwash.